Ocean Engineering 71 (2013) 17–27

Contents lists available at ScienceDirect

Ocean Engineering

journal homepage: www.elsevier.com/locate/oceaneng

Towards a global regionally varying allowance for sea-level rise

J.R. Hunter [a,*], J.A. Church [b], N.J. White [b], X. Zhang [b]

[a] Antarctic Climate & Ecosystems Cooperative Research Centre, Private Bag 80, Hobart, Tasmania 7001, Australia
[b] Centre for Australian Weather and Climate Research and Wealth from Oceans Flagship, CSIRO Marine and Atmospheric Research, GPO Box 1538, Hobart, Tasmania 7000, Australia

ARTICLE INFO

Available online 31 January 2013

Keywords:
Sea-level rise
Storm tide
Climate change
Climate projection

ABSTRACT

Allowances have been developed for future rise of relative sea-level (i.e. sea level relative to the land) based on the projections of regional sea-level rise, its uncertainty, and the statistics of tides and storm surges (storm tides). An 'allowance' is, in this case, the vertical distance that an asset needs to be raised under a rising sea level, so that the present likelihood of flooding does not increase. This continues the work of Hunter (2012), which presented allowances based on global-average sea level and local storm tides. The inclusion of regional variations of sea-level rise (and its uncertainty) significantly increases the global spread of allowances. For the period 1990–2100 and the A1FI emission scenario (which the world is broadly following at present), these range from negative allowances caused by land uplift (in the northern regions of North America and Europe) to the upper 5-percentile which is greater than about 1 m (e.g. on the eastern coastline of North America).

1. Introduction

A major effect of climate change is a present and continuing increase in sea level, caused mainly by thermal expansion of seawater and the addition of water to the oceans from melted land ice (e.g. Meehl et al., 2007, as reported in the Fourth Assessment Report (AR4) of the Intergovernmental Panel on Climate Change (IPCC)). Over the last two decades, the rate of global-average sea-level rise was about 3.2 mm yr^{-1} (Church and White, 2011). At the time of AR4 in 2007, sea level was projected to rise at a maximum rate of about 10 mm yr^{-1} and to a maximum level of about 0.8 m (relative to 1990) by the last decade of the 21st century, in the absence of significant mitigation of greenhouse-gas emissions (Meehl et al., 2007, Table 10.7, including 'scaled-up ice sheet discharge').

Sea-level rise, like the change of many other climate variables, will be experienced mainly as an increase in the frequency or likelihood (probability) of extreme events, rather than simply as a steady increase in an otherwise constant state. One of the most obvious adaptations to sea-level rise is to raise an asset (or its protection) by an amount that is sufficient to achieve a required level of precaution. The selection of such an allowance has often, unfortunately, been quite subjective and qualitative, involving concepts such as 'plausible' or 'high-end' projections. Hunter (2012) described a simple technique for estimating an allowance for sea-level rise using extreme-value theory. This allowance ensures that the expected, or average, number of extreme (flooding) events in a given period is preserved. In other words, any asset raised by this allowance would experience the same frequency of flooding events under sea-level rise as it would without the allowance and without sea-level rise. It is important to note that this allowance only relates to the effect of sea-level rise on *inundation* and *not* on the recession of soft (e.g. sandy) shorelines or on other impacts.

Under conditions of uncertain sea-level rise, the 'expected number of flooding events in a given period' is here defined in the following way. It is supposed that there are n possible futures, each with a probability, P_i, of being realised. For each of these futures, the expected number of flooding events in a given period is given by N_i. The effective, or overall, expected number of flooding events (considering all possible futures) is then considered to be $\sum_{i=1}^{n} P_i N_i$, where $\sum_{i=1}^{n} P_i = 1$.

In the terminology of risk assessment (e.g. ISO, 2009), the expected number of flooding events in a given period is known as the *likelihood*. If a specific cost may be attributed to one flooding event, then this cost is termed the *consequence*, and the combined effect (generally the product) of the likelihood and the consequence is the *risk* (i.e. the total effective cost of damage from flooding over the given period). The allowance is the height that an asset needs to be raised under sea-level rise in order to keep the flooding likelihood the same. If the cost, or consequence, of a single flooding event is constant than this also preserves the flooding risk.

An important property of the allowance is that it is *independent of the required level of precaution* (when measured in terms of *likelihood* of flooding). In the case of coastal infrastructure, an appropriate

* Corresponding author. Tel.: +61 4 2709 8831; fax: +61 3 6226 2440.
E-mail addresses: jrh@johnroberthunter.org (J.R. Hunter), John.Church@csiro.au (J.A. Church), Neil.White@csiro.au (N.J. White), Xuebin.Zhang@csiro.au (X. Zhang).

0029-8018/$ - see front matter © 2013 Elsevier Ltd. All rights reserved.
http://dx.doi.org/10.1016/j.oceaneng.2012.12.041

height should first be selected, based on *present* conditions and an acceptable degree of precaution (e.g. an average of one flooding event in 100 years). If this height is then raised by the allowance calculated for a specific period, the required level of precaution will be sustained until the end of this period.

The method assumes that there is no change in the variability of the extremes (specifically, the scale parameter of the Gumbel distribution; see Section 2). In other words, the statistics of tides and storm surges (storm tides) relative to mean sea level are assumed to be unchanged. It is also assumed that there is no change in wave climate (and therefore in wave setup and runup). The allowance derived from this method depends also on the distribution function of the uncertainty in the rise in mean sea level at some future time. However, once this distribution and the Gumbel scale parameter has been chosen, the remaining derivation of the allowance is entirely objective.

If the future sea-level rise were known exactly (i.e. the uncertainty was zero), then the allowance would be equal to the central value of the estimated rise. However, because of the exponential nature of the Gumbel distribution (which means that overestimates of sea-level rise more than compensate for underestimates of the same magnitude), uncertainties in the projected rise *increase* the allowance above the central value.

Hunter (2012) combined the Gumbel scale parameters derived from 198 tide-gauge records in the *GESLA* (Global Extremes Sea-Level Analysis) database (see Menéndez and Woodworth, 2010) with projections of global-average sea-level rise, in order to derive estimates of the allowance around much of the world's coastlines. The spatial variation of this allowance therefore depended only on variations of the Gumbel scale parameter. We here derive improved estimates of the allowance using the same *GESLA* tide-gauge records, but spatially varying projections of sea level from the IPCC AR4 (Meehl et al., 2007) with enhancements to account for glacial isostatic adjustment (GIA), and ongoing changes in the Earth's loading and gravitational field (Church et al., 2011). We use projections for the A1FI emission scenario (which the world is broadly following at present; Le Quéré et al., 2009).

The results presented here relate to an approximation of *relative sea level* (i.e. sea level relative to the land). They include the effects of vertical land motion due to changes in the Earth's loading and gravitational field caused by past and ongoing changes in land ice. They do not include effects due to local land subsidence produced, for example, by deltaic processes or groundwater withdrawal; *separate allowances should be applied to account for these latter effects*.

A fundamental problem with existing sea-level rise projections is a lack of information on the upper bound for sea-level rise during the 21st century, in part because of our poor knowledge of the contribution from ice sheets (IPCC, 2007). This effectively means that the likelihood of an extreme high sea-level rise (the upper tail of the distribution function of the sea-level rise uncertainty) is poorly known. The results described here are based on relatively thin-tailed distributions (normal and raised cosine) and may therefore not be appropriate if the distribution is fat-tailed (Section 6). For cases where consequence of flooding would be 'dire' (in the sense that the consequence of flooding would be unbearable, no matter how low the likelihood), a more appropriate allowance would be based on the best estimate of the maximum possible rise.

2. Theory

Extremes are generally described by *exceedance events* which are events which occur when some variable exceeds a given level. Two statistics are conventionally used to describe the likelihood of extreme events such as flooding from the ocean. These are the *average recurrence interval* (or *ARI*), R, and the *exceedance probability*, E, for a given period, T. The ARI is the average period between extreme events (observed over a long period with many events), while the exceedance probability is the probability of at least one exceedance event happening during the period T. Exceedance distributions are often expressed in terms of the *cumulative distribution function*, F, where $F=1-E$. F is just the probability that there will be *no* exceedances during the prescribed period, T. These statistics are related by (e.g. Pugh, 1996)

$$F=1-E=\exp\left(-\frac{T}{R}\right)=\exp(-N) \tag{1}$$

where N is the expected, or average, number of exceedances during the period T.

Eq. (1) involves the assumption (made throughout this paper) that exceedance events are independent; their occurrence therefore follows a Poisson distribution. This requires a further assumption about the relevant time scale of an event. If multiple closely spaced events have a single cause (e.g. flooding events caused by one particular storm), they are generally combined into a single event using a declustering algorithm.

The occurrence of sea-level extremes, and therefore, the ARI and the exceedance probability, will be modified by sea-level rise, the future of which has considerable uncertainty. For example, the projected sea-level rise for 2090–2099 relative to 1980–1999, for the A1FI emission scenario (which the world is broadly following at present; Le Quéré et al., 2009), is 0.50 ± 0.26 m (5–95% range, including scaled-up ice sheet discharge; Meehl et al., 2007), the range being larger than the central value.

The expected number of exceedances above a given level and over a given period may, in general, be described by

$$N=\mathcal{N}\left(\frac{\mu-z_P}{\lambda}\right) \tag{2}$$

where $\mathcal{N}$ is some general dimensionless function, z_P is the physical height (e.g. the height of a critical part of the asset), μ is a 'location parameter' and λ is a 'scale parameter'. As noted in Section 1, it is assumed that there is no change in the variability of the extremes, which implies that the scale parameter, λ, does not change with a rise in sea level.

Mean sea level is now raised by an amount $\Delta z+z'$, where Δz is the central value of the estimated rise and z' is a random variable with zero mean and a distribution function, $P(z')$, to be chosen below. This effectively increases the location parameter, μ, by $\Delta z+z'$. At the same time, the asset is raised by an allowance, a, so that it is now located at a height z_P+a. Under these conditions of (uncertain) sea-level rise and raising of the asset, the overall (or effective) expected number, N_{ov}, of exceedances ($>z_P+a$) during the period T, becomes

$$N_{ov}=\int_{-\infty}^{\infty}P(z')\mathcal{N}\left(\frac{\mu-z_P+\Delta z+z'-a}{\lambda}\right)dz' \tag{3}$$

The function, $\mathcal{N}$, is often well-fitted by a *generalised extreme-value distribution* (*GEV*). The simplest of these, the *Gumbel* distribution, fits most sea-level extremes quite well (e.g. van den Brink and Können, 2011). The Gumbel distribution may be expressed as (e.g. Coles, 2001, p. 47)

$$F=\exp\left(-\exp\left(\frac{\mu-z_P}{\lambda}\right)\right) \tag{4}$$

where F is the probability that there will be no exceedances $>z_P$ during the prescribed period, T.

From Eqs. (1), (2) and (4)

$$N=\mathcal{N}\left(\frac{\mu-z_P}{\lambda}\right)=\exp\left(\frac{\mu-z_P}{\lambda}\right) \tag{5}$$

μ is therefore the value of z_P for which $N=1$ during the period T, and λ, the 'scale parameter', is an e-folding distance in the vertical. Globally, the scale parameter has a quite narrow range;

for the sea-level records described in Section 4, the 5-percentile, median and 95-percentile values of the scale parameter are 0.05 m, 0.12 m and 0.19 m, respectively.

Again, as noted in Section 1, it is assumed that the scale parameter, λ, does not change with a rise in sea level. It will also be noted later (Section 6) that Eq. (5) is only valid over the restricted range of z_P that encompasses the high extreme values.

Eq. (3) therefore becomes (Hunter, 2012):

$$N_{ov} = \int_{-\infty}^{\infty} P(z') \exp\left(\frac{\mu - z_P + \Delta z + z' - a}{\lambda}\right) dz'$$
$$= N \exp\left(\left(\Delta z + \lambda \ln\left(\int_{-\infty}^{\infty} P(z') \exp\left(\frac{z'}{\lambda}\right) dz'\right) - a\right)/\lambda\right) \quad (6)$$

In order to preserve the expected number of exceedances (or flooding events), we require that $N_{ov} = N$. Therefore, the allowance, a, is equal to the term $\Delta z + \lambda \ln(\cdots)$ in the last part of Eq. (6). This allowance is composed of two parts: the mean sea-level rise, Δz, and the term $\lambda \ln(\cdots)$, which arises from the uncertainty in future sea-level rise. Hunter (2012) evaluated the allowance for three types of uncertainty distribution for future sea-level rise: a normal distribution, a boxcar (uniform) distribution and a raised cosine distribution. The resulting allowances may all be expressed as simple analytical expressions, involving the Gumbel scale parameter, λ, the central value of the estimated rise, Δz, and its standard deviation, σ. We here estimate the allowances using normal and raised cosine distributions, the former having fatter tails and therefore yielding higher allowances (the raised-cosine distribution falls to zero at a finite distance from the central value, the total range of the distribution being about 1.7 times the 5- to 95-percentile range). Both distributions were fitted to the 5- and 95-percentile range of the IPCC AR4 projections of sea-level rise, with the central value, Δz, being the mean of the 5- and 95-percentile values.

For a normal uncertainty distribution of future sea-level rise, the allowance is given by $\Delta z + \sigma^2/(2\lambda)$ (Hunter, 2012). A typical sea-level rise projection for 2100 relative to 1990 for the A1FI emission scenario is 0.5 ± 0.2 (standard deviation) m, and a typical Gumbel scale parameter is 0.1 m. In this case, the allowance is equal to 0.5 m (the mean sea-level rise) + 0.2 m (associated with the uncertainty) = 0.7 m, which is significant larger than the mean sea-level rise. However, in general, the allowance is less than the 95-percentile upper limit (which is 0.83 m in this typical case).

3. Projections of regional sea-level rise

Projections of the future climate are based on models driven by plausible scenarios for the emissions of greenhouse gases. In the case of the IPCC AR4 and the projections to be described in this section, emissions were based on the Special Report on Emission Scenarios (SRES; Nakicenovic et al., 2000).

The derivation of the projections of regional sea-level rise followed Church et al. (2011) and Slangen et al. (2012), and is described in detail in Appendix A. The resultant projections are composed of terms due to

1. the global-average sea-level rise (including 'scaled-up ice sheet discharge' (Meehl et al., 2007; see Fig. 1)),
2. spatially varying 'fingerprints' to account for changes in the loading of the Earth and in the gravitational field, in response to ongoing changes in land ice (Mitrovica et al., 2001, 2011),
3. glacial isostatic adjustment (GIA; Kendall et al., 2005) (GIA is the result of changes in the Earth's loading and gravitational field caused by past changes in land ice (predominantly, the most recent deglaciation from about 20,000 years ago). The northern regions of North America and Europe show significant uplift, which may lower relative sea level (i.e. sea level relative to the land) by as much as 20 mm yr^{-1}. In contrast, the eastern coastline of North America is sinking and shows positive GIA contributions as large as 2 mm yr^{-1}), and
4. spatially varying sea-level change due to change in ocean density and dynamics (e.g. Meehl et al., 2007, Section 10.6.2 and Fig. 10.32).

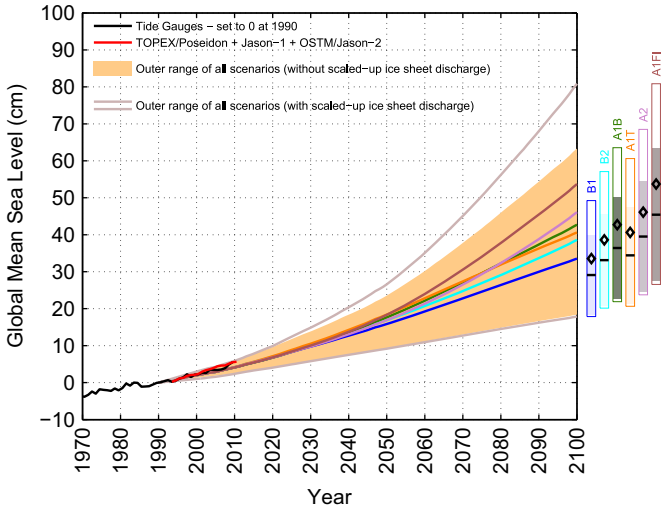

Fig. 1. Global-average projections of sea-level rise relative to 1990, based on the IPCC AR4 (Meehl et al., 2007) and reproduced in Church et al. (2011). The outer light lines and the shaded region show the 5- to 95-percentile range of projections with and without 'scaled-up ice sheet discharge' (SUISD), respectively. The continuous coloured lines from 1990 to 2100 indicate the central value of the projections, with SUISD. The open and shaded bars at the right show the 5- to 95-percentile range of projections for 2100 for the various SRES scenarios, with and without SUISD. The diamonds and horizontal lines in the bars are the central values with and without SUISD. The observational estimates of global-average sea level based on tide-gauge measurements and satellite altimeter data are shown in black and red, respectively. The tide-gauge data are set to zero at the start of the projections in 1990, and the altimeter data are set equal to the tide-gauge data at the start of the record in 1993. (For interpretation of the references to color in this figure legend, the reader is referred to the web version of this article.)

While terms (2) and (3) are generated by effectively the same models of crustal loading and gravitational field, they are forced by quite different time-series of land-ice change. It should also be noted that the terms (1)–(4) have been generated by separate models and are added linearly; nonlinear interactions between the terms are ignored.

The spatially varying sea-level rise related to change in ocean density and dynamics (term (4), above) is provided by atmosphere–ocean general circulation models (AOGCMs). While global-average sea-level rise has been reported for six emission scenarios (B1, B2, A1B, A1T, A2, A1FI; Meehl et al., 2007), results from AOGCMs are only available for scenarios B1, A1B and A2. For estimating spatially varying projections for A1FI (the highest of the SRES scenarios), the central values and uncertainties derived from combining terms (1)–(4), above, were scaled using ratios of the global-average projections for A1FI and A2.

4. Statistics of storm tides

The scale parameter, λ, was estimated from the *GESLA* (Global Extreme Sea-Level Analysis) sea-level database (see Menéndez and Woodworth, 2010) which has been collected through a collaborative activity of the Antarctic Climate & Ecosystems Cooperative Research

Centre, Australia, and the National Oceanography Centre Liverpool (NOCL), UK. The data covers a large portion of the world and is sampled at least hourly (except where there are data gaps). The database was downloaded from NOCL on 26 October 2010 and contains 675 files. However, many of these files are near-duplicates provided by different agencies. Many are also as short as one or two years and are therefore not suitable for the analysis of extremes (it is generally considered that ARIs of up to about four times the record length may be derived from tide-gauge records (e.g. Pugh, 1996) so that, for example, the estimation of 100-year ARIs requires records of at least 25 years duration). Hunter (2012) performed initial data processing, resulting in 198 tidal records, each of which was at least 30 years long. However, one of these is from Trieste in the Mediterranean, which is poorly resolved by the ocean components of the AOGCMs (the Mediterranean is omitted altogether from Meehl et al., 2007, Fig. 10.32, which shows the projected spatially varying sea-level change due to change in ocean density and dynamics). The data from Trieste was not therefore used in the present analysis, which is therefore based on 197 global sea-level records.

Prior to extreme analysis, the data was 'binned', so as to produce files with a minimum sampling interval of one hour, and detrended. Annual maxima were estimated using a declustering algorithm such that any extreme events closer than 3 days were counted as a single event, and any gaps in time were removed from the record. These annual maxima were then fitted to a Gumbel distribution using the *ismev* package (Coles, 2001, p. 48) implemented in the statistical language *R* (R Development Core Team, 2008). This yielded the scale parameter, λ, for each of the 197 records. It is assumed that λ does not change in time.

5. Regional allowances

Allowances for future sea-level rise have generally been based on global-average projections, without adjustment for regional variations (which are related to the land-ice fingerprint, GIA, and change in ocean density and dynamics). Fig. 2 shows the vertical allowance for sea-level rise from 1990 to 2100 for the A1FI emission scenario, at each of the 197 tide-gauge locations. The allowance is based on the global-average rise in mean sea level and on the statistics of storm tides observed at each location (Section 4). The uncertainty in the projections of sea-level rise was fitted to a normal distribution. The use of a raised-cosine distribution, which has thinner tails, yields a smaller allowance. Fig. 2 shows effectively the same information as Fig. 4 of Hunter (2012), except for being based on a slightly different projection of mean sea-level rise. Fig. 3 shows the cumulative distribution function for these allowances, for normal and raised-cosine uncertainty distributions, constructed from the 197 tide-gauge allowances. Figs. 2 and 3 show that the allowances have only a small variation, 90% falling within the ranges 0.61–0.79 m and 0.61–0.73 m, for normal and raised-cosine uncertainty distributions, respectively. The difference between allowances based on normal and raised-cosine uncertainty distributions increases monotonically with the allowance, reaching a maximum of about 0.18 m (in accordance with the results of Eq. (6), with constant Δz, variable λ, and $P(z')$ chosen as normal or raised-cosine distributions).

Figs. 4 and 5 show the same information as Figs. 2 and 3 but with the global-average rise in mean sea level replaced by a spatially varying rise. The allowance is therefore based on a spatially varying rise in mean sea level (Section 3) and on the statistics of storm tides observed at each location (Section 4). Fig. 5 shows that, for a given probability, the difference between using normal and raised-cosine uncertainty distributions is at most about 0.08 m, but it should be noted that, due to the spatial variation in the sea-level rise projections, the difference at any one location may be larger than this. A striking feature of Fig. 5 is the relatively large number of sites (about 4.5%) with negative allowances (these are all indicated by

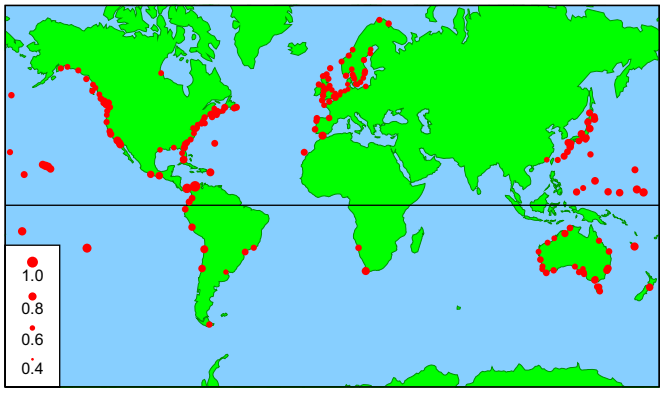

Fig. 2. *Allowances using global-average sea-level rise.* Vertical allowances (m) for sea-level rise from 1990 to 2100 for the A1FI emission scenario, indicated by the dot diameter. The allowances are based on a global-average rise in mean sea level, derived from the IPCC AR4, and on the statistics of storm tides observed at each location. The uncertainty in the projections of sea-level rise was fitted to a normal distribution.

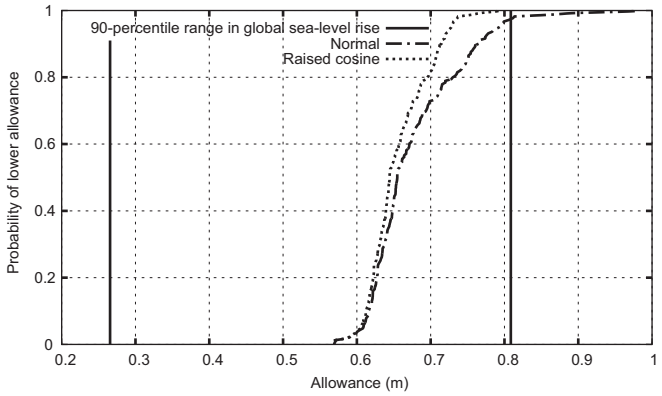

Fig. 3. *Allowances using global-average sea-level rise.* Cumulative distribution function for vertical allowances for sea-level rise from 1990 to 2100 for the A1FI emission scenario, estimated from 197 tide-gauge locations, for normal and raised-cosine uncertainty distributions. The allowances are based on a global-average rise in mean sea level, derived from the IPCC AR4, and on the statistics of storm tides observed at each location. Also shown is the 90-percentile (5- to 95-percentile) range of the global-average rise in mean sea level, from the IPCC AR4.

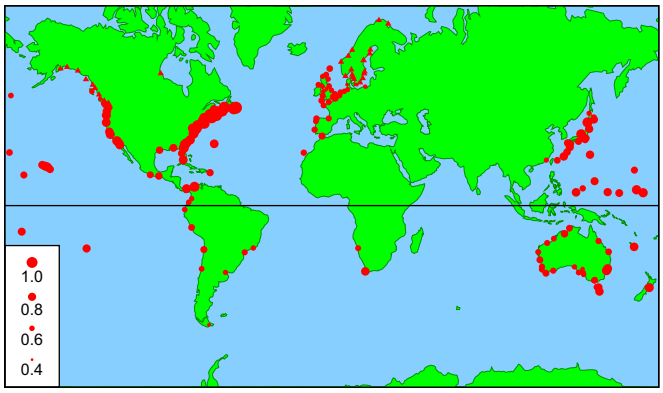

Fig. 4. *Allowances using spatially varying sea-level rise.* Vertical allowances (m) for sea-level rise from 1990 to 2100 for the A1FI emission scenario, indicated by the dot diameter. The allowances are based on a spatially varying rise in mean sea level, and on the statistics of storm tides observed at each location. The uncertainty in the projections of sea-level rise was fitted to a normal distribution. Filled triangles indicate allowances less than 0.4 m.

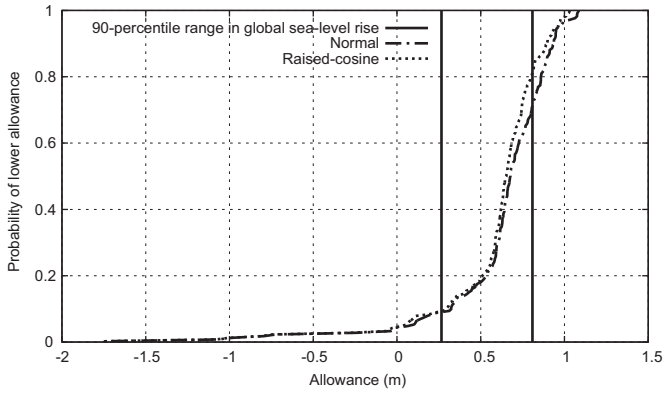

Fig. 5. *Allowances using spatially varying sea-level rise.* Cumulative distribution function for vertical allowances for sea-level rise from 1990 to 2100 for the A1FI emission scenario, estimated from 197 tide-gauge locations, for normal and raised-cosine uncertainty distributions. The allowances are based on a spatially varying rise in mean sea level, and on the statistics of storm tides observed at each location. Also shown is the 90-percentile (5- to 95-percentile) range of the global-average rise in mean sea level, from the IPCC AR4. It should be noted that the horizontal scale is quite different from the scale used in Fig. 3.

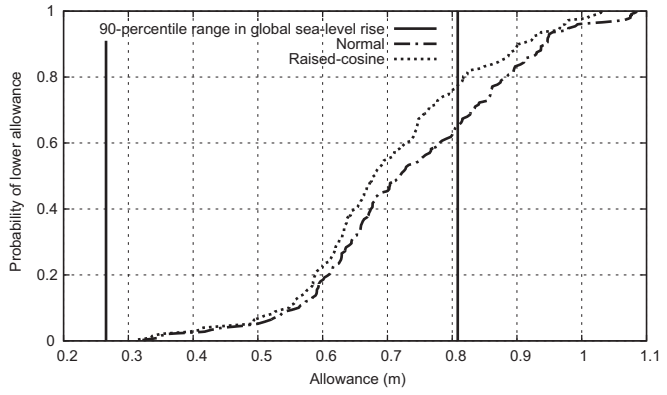

Fig. 6. As Fig. 5 but excluding all locations north of latitude 55° North.

filled triangles in Fig. 4, which denote allowances less than 0.4 m). Some of these (in the northern regions of North America and Europe) are caused by strongly negative GIA (land uplift), while the remainder (in the northwest region of North America) are caused by present changes in glaciers and icecaps. The top 5% of the locations have allowances greater than 0.97 m and 0.95 m for normal and raised-cosine uncertainty distributions, respectively.

Sites with negative or small positive allowances may be removed by excluding all locations north of latitude 55° North, as shown in Fig. 6, which is otherwise similar to Fig. 5. Rejecting these locations makes little difference to the top 5% of the remaining locations, which have allowances greater than 0.98 m and 0.97 m for normal and raised-cosine uncertainty distributions, respectively.

The results for each location and for a spatially varying sea-level rise are summarised in Appendix B, which shows allowances for the A1FI emission scenario, and for periods 1990–2100 and 2010–2100 (the latter being the more appropriate for present-day planning and policy decisions). The projections of sea-level rise used to derive these allowances were fitted to a normal distribution.

6. Applicability of the allowance and the problem of a fat upper tail

As noted in Section 1, a fundamental problem with existing sea-level rise projections is a lack of information on the upper bound for sea-level rise during the 21st century, in part because of our poor knowledge of the contribution from ice sheets (IPCC, 2007). This effectively means that the likelihood of an extreme high sea-level rise (the upper tail of the distribution function of the sea-level rise uncertainty) is poorly known.

The allowance depends on the Gumbel distribution, which only describes extreme events. Eq. (5) therefore only applies to the range of z_P that encompasses the high sea-level extremes. The allowance is therefore valid in cases where the uncertainty distribution of sea-level rise, $P(z')$, spans only the portion of $\mathcal{N}((\mu-z_P+\Delta z+z'-a)/\lambda)$ (Eq. (3)) that fits a Gumbel distribution. This is generally satisfied if $P(z')$ has thin tails (e.g. it is normal or raised-cosine). For the A1FI emission scenario and the period 1990–2100, the 5- to 95-percentile range spans 0.54 m, which is typically five times the scale parameter, λ, a range which the Gumbel distribution will generally cover satisfactorily.

However, if $P(z')$ had a fat upper tail, the distributions used here (normal and raised-cosine) would underestimate the allowance by not including the contribution from the tail in the integral in Eq. (3). This problem may be examined in terms of both *likelihood*, $\mathcal{N}$, and *risk*. In general, risk may be treated in the same way as likelihood, so that the analogue of Eq. (2) is

$$R=\mathcal{R}\left(\frac{\mu-z_P}{\lambda}\right) \tag{7}$$

and the analogue of Eq. (3) is

$$R_{ov}=\int_{-\infty}^{\infty}P(z')\mathcal{R}\left(\frac{\mu-z_P+\Delta z+z'-a}{\lambda}\right)dz' \tag{8}$$

where R is the risk and $\mathcal{R}$ is some general dimensionless function.

If the consequence of each flooding event is a constant, c, then $\mathcal{R}=c\mathcal{N}$ and $R_{ov}=cN_{ov}$. In this case, any allowance that preserves the overall *likelihood*, N_{ov}, also preserves the overall *risk*, R_{ov}.

There is one situation where fat-tailed $P(z')$ *may not* significantly influence the overall *likelihood*, and another where it may not significantly influence the overall *risk*.

Firstly, $\mathcal{N}((\mu-z_p+\Delta z+z'-a)/\lambda)$ may be less than the value given by a Gumbel distribution at large values of $(\mu-z_p+\Delta z+z'-a)/\lambda$, thereby reducing the effect of a fat upper tail in $P(z')$ on the overall likelihood, $\mathcal{N}_{ov}$ (Eq. (3)). A trivial (and extreme) example of this is where the fat upper tail spans the range in which the asset lies between mean sea level and the minimum high water level (e.g. mean high water neaps). Within this range, $\mathcal{N}$ is approximately constant at about one or two flooding events per day (for diurnal and semidiurnal tides, respectively); i.e. in this range the flooding likelihood, $\mathcal{N}$ does not increase with z', and the contribution of the fat upper tail to the overall likelihood N_{ov} may be small or negligible.

Secondly, even if the overall likelihood, N_{ov}, increases significantly due to a fat upper tail in $P(z')$, it is quite possible that the consequence of each flooding event decreases under these conditions, so that the overall *risk*, R_{ov}, is not dominated by the fat tail. A simple example of this is where the consequence is just the cost of rebuilding after each flooding event. When the likelihood (or frequency) of flooding events gets so large that rebuilding becomes impracticable, the risk becomes constant and roughly equivalent to the cost of abandoning the location altogether. In this case, $\mathcal{R}$ does not increase with z', and the contribution of the fat upper tail to the overall risk R_{ov} may be small or negligible.

The determination of the total *risk* resulting from a probability distribution with a poorly known upper tail (in this case, $P(z')$), combined with a function which may increase exponentially in the direction of the tail (in this case, $\mathcal{N}$ or $\mathcal{R}$) is non-trivial, and is the subject of some debate. In a related problem (the economic implications of projections of global temperature), Weitzman

(2009) introduced a 'dismal theorem' which suggested that the effective risk associated with fat tails could become infinite, although subsequent papers (e.g. Nordhaus, 2011; Pindyck, 2011) have argued that the conditions for the validity of the 'dismal theorem' are quite restrictive.

Luckily, there is good reason to believe that the probability distribution of future sea-level rise is bounded. On a millennial scale, if all the ice and snow on land were transferred to the ocean, the rise would be limited to about 64 m (Lemke et al., 2007), and Pfeffer et al. (2008) has estimated an upper bound for sea-level rise for the 21st century of 2.0 m. Given that the detailed shape of the uncertainty distribution is largely unknown, a precautionary approach in cases where the consequence of flooding would be 'dire' (in the sense that the consequence of flooding would be unbearable, no matter how low the likelihood) is to choose an allowance based on the best estimate of the maximum possible rise (an example being the Netherlands, where coastal flood planning is based on an ARI of 10,000 years Maaskant et al., 2009). However, in other cases, where the consequences of unforeseen flooding events (i.e. 'getting the allowance wrong') are manageable, the allowance presented here represents a practical solution to planning for sea-level rise while preserving an acceptable level of likelihood or risk.

7. Discussion and conclusions

A vertical allowance for sea-level rise has been defined such that any asset raised by this allowance would experience the same frequency of flooding events under sea-level rise as it would without the allowance and without sea-level rise (Hunter, 2012). Allowances have been evaluated by combining spatially varying projections of sea-level rise with the statistics of observed storm tides at 197 tide-gauge sites. These allowances relate to the A1FI emission scenario, and the periods 1990–2100 and 2010–2100 (the latter being the more appropriate for present-day planning and policy decisions). We use the A1FI emission scenario because this is the one that the world is broadly following at present (Le Quéré et al., 2009). It must, however, be emphasised that the choice of emission scenario represents a major additional source of uncertainty, the central value of the 1990–2100 projection for the highest SRES scenario (A1FI) being about 60% larger than the projection for the lowest SRES scenario (B1).

Two uncertainty distributions were used (normal and raised-cosine); Figs. 2 and 4, and Appendix B, show the results for a normal distribution which has fatter tails and which yields a slightly higher allowance.

Planning allowances have typically been selected by choosing a specific percentile of a projection of future global-average sea-level rise. Often the 95-percentile upper limit, which is the one provided by the IPCC AR4 (Meehl et al., 2007), has been chosen. However, as shown in Fig. 3 (for the period 1990–2100), if sea-level rise were globally uniform, an allowance equal to the 95-percentile limit is generally significantly larger than would be required to preserve the frequency of flooding events under sea-level rise; for the period 1990–2100, only 2.6% of the locations considered have allowances greater than the 95-percentile upper limit. The spread of allowances in Fig. 3 is entirely due to spatial variations in the statistics of storm tides (specifically, the Gumbel scale parameter).

When the spatial variation of projected sea-level rise (due to ongoing changes in the Earth's loading and gravitational field, thermal expansion, ocean dynamics and GIA) is included, the distribution of the allowances widens significantly (Fig. 5, for the period 1990–2100). This widening is related to locations (in northern regions of North America and Europe) which experience strongly negative GIA, and others (in the northwest region of North America) which are influenced by present changes in glaciers and icecaps. These processes contribute a significant fall in sea level, leading to negative 'allowances', some of which are less than -1 m. The spread of allowances covers the entire 90-percentile range of the A1FI projections of global-average sea-level rise, with 9% of the locations having allowances less than the 5-percentile lower limit and 29% of the locations having allowances greater than the 95-percentile upper limit.

Fig. 4 shows the global distribution of the allowances for the period 1990–2100. Obvious features are the low and negative allowances in the northern regions of North America and Europe (where the land is rising due to GIA and to present changes in glaciers and icecaps), and higher allowances along the eastern coastline of North America (where the land is sinking, again due to GIA).

Appendix B provides a table of allowances for the periods 1990–2100 and 2010–2100. These may be used as a starting point for the determination of allowances for planning and policy decisions. However, the following caveats should be recognised:

1. The determination of allowances given in this paper is based on the assumption that the Gumbel scale parameter (and hence the variability of the storm tides) will not change in time. This is supported by the fact that present evidence (Bindoff et al., 2007; Lowe et al., 2012; Menéndez and Woodworth, 2010; Woodworth and Blackman, 2004) suggests that the rise in mean sea level is generally the dominant cause of any observed increase in the frequency of extreme events. In addition, using model projections of storm tides in southeast Australia to 2070, McInnes et al. (2009) showed that the increase in the frequency of flooding events was dominated by sea-level rise.
2. The allowance includes no contribution due to possible changes in wave setup or runup.
3. The allowance includes no contribution due to the change in tides caused by sea-level rise, which are generally small and confined to quite specific locations in shelf seas (e.g. Pickering et al., 2012).
4. The allowance depends on the shape of the distribution of the uncertainty of the projections of mean sea-level rise. Two distributions have been considered here: a normal and a raised-cosine distribution. The raised-cosine distribution, which is limited to about 1.7 times the 5- to 95-percentile range (it is zero outside these limits), was included because of the arguments for an upper bound to the rate of sea-level rise (Pfeffer et al., 2008). For spatially varying sea-level rise, the allowances based on normal and raised-cosine distributions differ by about 0.08 m at most, the normal distribution giving the larger allowance. However, the possibility of the uncertainty distribution having fatter tails than a normal distribution has been considered (Section 6). Unfortunately the IPCC AR4 gives no guidance as to the choice of an appropriate uncertainty distribution, nor any indication of an 'upper bound for sea-level rise' (IPCC, 2007), and we have here based our allowances in Figs. 2 and 4, and in Appendix A, on the normal distribution. These allowances represent a practical solution to planning for sea-level rise while preserving an acceptable level of flooding likelihood, in cases where 'getting the allowance wrong' is manageable. However, in cases where the consequence of flooding would be 'dire' (in the sense that the consequence of flooding would be unbearable, no matter how low the likelihood, as in the case of the Netherlands), a precautionary approach is to choose an allowance based on the best estimate of the maximum possible rise.
5. The projections of the IPCC AR4 apparently relate to the *spread* of model projections (akin to the *standard deviation*) rather than to

the uncertainty (akin to the *standard error*) of the best estimate of the projections. The metric of uncertainty, σ (see Section 2), strictly relates to the *standard error*. However, for reasons discussed by Hunter (2012), σ is here associated with the *standard deviation* (rather than the *standard error*) of the projections.

There are therefore significant unknowns associated with the shape and extent of the uncertainty distribution of the projections of sea-level rise. Improved allowances for sea-level rise require better estimates of future sea level and, just as importantly, of its uncertainty distribution and the behaviour of its upper tail.

Appendix A. The derivation of regionally varying sea-level rise projections

Projections of regional relative sea-level rise were derived as in Church et al. (2011) and consist of

$$\Delta P(x,y,t) = \Delta S(t) + \Delta R(t) + \Delta F(x,y,t) + \Delta A(x,y,t) + \Delta D(x,y,t) \quad (A.1)$$

where $\Delta P(x,y,t)$ is the spatially and temporally varying projection of regional relative sea-level rise, x and y are the horizontal spatial coordinates, t is the time, and

1. $\Delta S(t)$ is the global-average sea-level rise, based on the best-available modelling at the time of the IPCC AR4. This term is consistent with the sixth row (labelled 'Sea level rise') of Table 10.7 of Meehl et al. (2007). It is composed of

   $$\Delta S(t) = \Delta S_T(t) + \Delta S_I(t) + \Delta S_G(t) + \Delta S_A(t) \quad (A.2)$$

   where $\Delta S_T(t)$ is the contribution from thermal expansion (consistent with the first row of Meehl et al. (2007, Table 10.7)). $\Delta S_I(t)$, $\Delta S_G(t)$ and $\Delta S_A(t)$ are contributions due to melting ice from 'glaciers and ice caps', Greenland and Antarctica, respectively, estimated from surface mass balance; they are consistent with the second, third and fourth rows of Table 10.7 of Meehl et al. (2007).
   Annual time series of $\Delta S(t)$, and the 5- and 95-percentile uncertainty range, were obtained for emission scenarios B1, B2, A1B, A1T, A2 and A1FI (Gregory, pers. comm.). $\Delta S(t)$ is just the mean of the 5- and 95-percentile range, and we derived the uncertainty half-range, $\delta S(t)$, from half the difference between the 5- and 95-percentile values.
2. $\Delta R(t)$ is a component accounting for poorly quantified 'rapid dynamical changes' to land ice. This term is consistent with the seventh row (labelled 'Scaled-up ice sheet discharge') of Table 10.7 of Meehl et al. (2007). It was assumed that one-third of this comes from Greenland and two-thirds from West Antarctica. $\Delta R(t)$ was provided (Gregory, pers. comm.) and we derived the uncertainty, $\delta R(t)$ (the 5- to 95-percentile half-range), by assuming a coefficient of variation (the ratio of the standard deviation to the central value) of 0.677 (Gregory, pers. comm.) and converting from the standard deviation to the half-range by multiplying by 1.6448537 (assuming a normal distribution), so

   $$\delta R(t) = \Delta R(t) \times 0.677 \times 1.6448537 \quad (A.3)$$

3. $\Delta F(x,y,t)$ is a spatially and temporally varying 'fingerprint' term accounting for changes in the loading of the Earth and in the gravitational field, in response to ongoing changes in land ice (Mitrovica et al., 2001, 2011). It is composed of

   $$\begin{aligned}\Delta F(x,y,t) = {} & (F_I(x,y)-1)\Delta S_I(t) + (F_G(x,y)-1)\Delta S_G(t) \\ & + (F_A(x,y)-1)\Delta S_A(t) + 0.333(F_G(x,y)-1)\Delta R(t) \\ & + 0.667(F_W(x,y)-1)\Delta R(t)\end{aligned} \quad (A.4)$$

   where $F_I(x,y)$, $F_G(x,y)$, $F_A(x,y)$ and $F_W(x,y)$ are 'fingerprints' for ice loss from 'glaciers and ice caps', Greenland, Antarctica as a whole, and West Antarctica, respectively, and:

   $$\overline{F_I(x,y)} = 1, \quad \overline{F_G(x,y)} = 1, \quad \overline{F_A(x,y)} = 1, \quad \overline{F_W(x,y)} = 1 \quad (A.5)$$

   where the overbar indicates a global average, so that the global-average of each term in Eq. (A.4) is zero. The uncertainty, $\delta F(x,y,t)$, of this 'fingerprint' term was estimated from:

   $$\delta F(x,y,t) = \frac{|\Delta F(x,y,t)|\,\delta S(t)}{\Delta S(t)} \quad (A.6)$$

4. $\Delta A(x,y,t)$ is glacial isostatic adjustment or GIA from Kendall et al. (2005). This is spatially varying with a zero global-average:

   $$\overline{\Delta A(x,y,t)} = 0 \quad (A.7)$$

   $\Delta A(x,y,t)$ increases linearly with time. No uncertainty was estimated for this term.
5. $\Delta D(x,y,t)$ is a spatially and temporally varying term related to change in ocean density and dynamics (Meehl et al., 2007). This is expressed as the deviation of regional sea-level rise from the global average, so:

   $$\overline{\Delta D(x,y,t)} = 0 \quad (A.8)$$

   The uncertainty of this term, $\delta D(x,y,t)$, was estimated from the spread of simulations from different models.

The uncertainties in terms (1)–(3) were added linearly, and the result was added in quadrature to the error in term (5), in order to obtain the uncertainty, $\delta P(x,y,t)$, in $\Delta P(x,y,t)$:

$$\delta P(x,y,t) = \sqrt{(\delta S(t) + \delta R(t) + \delta F(x,y,t))^2 + (\delta D(x,y,t))^2} \quad (A.9)$$

The spatially and temporally varying sea-level rise related to change in ocean density and dynamics, $\Delta D(x,y,t)$, was provided by atmosphere–ocean general circulation models (AOGCMs). While global-average sea-level rise ($\Delta S(t) + \Delta R(t)$) has been estimated for six emission scenarios (B1, B2, A1B, A1T, A2, A1FI; Meehl et al., 2007), results from AOGCMs are only available for scenarios B1, A1B and A2. Spatially and temporally varying projections ($\Delta P(x,y,t)$, $\delta P(x,y,t)$) for B2, A1T and A1FI were here obtained by using the results for ($\Delta P(x,y,t)$, $\delta P(x,y,t)$) for the nearest adjacent projections for B1, A1B or A2, and scaling using ratios derived from the respective global-average projections ($\Delta S(t) + \Delta R(t)$, $\delta S(t) + \delta R(t)$). The present paper discusses A1FI projections derived from spatially varying A2 projections and global-average projections for A1FI and A2. Therefore (omitting the variables x, y and t, for clarity):

$$\Delta P(\mathrm{A1FI}) = \frac{\Delta P(\mathrm{A2})(\Delta S(\mathrm{A1FI}) + \Delta R(\mathrm{A1FI}))}{(\Delta S(\mathrm{A2}) + \Delta R(\mathrm{A2}))} \quad (A.10)$$

and

$$\delta P(\mathrm{A1FI}) = \frac{\delta P(\mathrm{A2})(\delta S(\mathrm{A1FI}) + \delta R(\mathrm{A1FI}))}{(\delta S(\mathrm{A2}) + \delta R(\mathrm{A2}))} \quad (A.11)$$

Appendix B. Summary of values for each location with a spatially varying sea-level rise and a normal distribution of uncertainty

The summary of locations, 5- to 95-percentile ranges of projections of mean sea-level rise, and allowances, for the periods 1990–2100 and 2010–2100 is given in Table B1.

Table B1
Summary of locations, 5- to 95-percentile ranges of projections of mean sea-level rise, and allowances, for the periods 1990–2100 and 2010–2100.

Site name	Longitude, latitude (deg.)	Projection 1990–2100 5,95% (m)	Projection 2010–2100 5,95% (m)	Allowance 1990–2100 (m)	Allowance 2010–2100 (m)
Abashiri	144.28, 44.02	0.09, 0.68	0.12, 0.64	0.59	0.53
Aberdeen	357.93, 57.14	0.04, 0.76	0.08, 0.70	0.62	0.55
Aburatsu	131.42, 31.57	0.24, 0.84	0.25, 0.76	0.68	0.60
Acapulco-A	260.09, 16.84	0.18, 0.77	0.22, 0.70	0.72	0.62
Adak	183.37, 51.86	0.15, 0.76	0.18, 0.67	0.63	0.54
Albany	117.88, −35.03	0.25, 0.82	0.25, 0.76	0.71	0.64
Alert Bay	233.07, 50.59	−0.08, 0.62	−0.03, 0.57	0.43	0.38
Antofagasta	289.60, −23.65	0.10, 0.71	0.12, 0.66	0.72	0.63
Argentia	306.02, 47.30	0.39, 1.14	0.32, 1.01	1.08	0.92
Astoria	236.23, 46.21	0.34, 0.99	0.32, 0.87	0.83	0.72
Atlantic City	285.58, 39.35	0.48, 1.16	0.46, 0.98	0.98	0.81
Balboa	280.43, 8.96	0.18, 0.75	0.20, 0.68	0.58	0.53
Baltimore	283.42, 39.27	0.43, 1.11	0.42, 0.95	0.91	0.77
Bamfield	234.86, 48.84	0.09, 0.81	0.11, 0.73	0.66	0.57
Bella Bella	231.86, 52.16	−0.15, 0.55	−0.09, 0.51	0.35	0.32
Bermuda	295.30, 32.40	0.28, 0.92	0.28, 0.81	0.84	0.71
Boston	288.95, 42.35	0.36, 1.12	0.32, 0.98	0.95	0.81
Brest	355.50, 48.38	0.19, 0.84	0.20, 0.76	0.64	0.58
Broome	122.22, −18.00	0.18, 0.83	0.19, 0.74	0.63	0.56
Buenaventura	282.90, 3.90	0.15, 0.71	0.17, 0.65	0.60	0.53
Buenos Aires	301.50, −34.67	0.12, 0.86	0.17, 0.69	0.59	0.48
Bunbury	115.63, −33.32	0.20, 0.83	0.21, 0.74	0.63	0.57
Bundaberg	152.38, −24.77	0.26, 0.82	0.25, 0.75	0.70	0.63
Burnie	145.92, −41.05	0.22, 0.81	0.22, 0.75	0.68	0.62
Calais	1.87, 50.97	0.17, 0.87	0.19, 0.79	0.72	0.64
Callao-B	282.85, −12.05	0.10, 0.73	0.14, 0.66	0.70	0.59
Campbell River	234.75, 50.04	−0.13, 0.57	−0.08, 0.53	0.36	0.33
Cananeia	312.07, −25.02	0.18, 0.75	0.16, 0.68	0.65	0.57
Cape May	285.04, 38.97	0.50, 1.18	0.48, 1.00	0.99	0.83
Carnarvon	113.62, −24.88	0.15, 0.83	0.18, 0.74	0.64	0.57
Cartagena	284.47, 10.38	0.22, 0.77	0.25, 0.67	0.95	0.72
Cascais	350.58, 38.69	0.18, 0.79	0.22, 0.71	0.67	0.58
Ceuta	354.68, 35.90	0.14, 0.72	0.17, 0.66	0.73	0.62
Charleston	280.07, 32.78	0.38, 1.04	0.36, 0.91	0.91	0.78
Charlottetown	296.88, 46.23	0.33, 1.13	0.29, 0.99	0.94	0.80
Cherbourg	358.38, 49.65	0.14, 0.80	0.16, 0.72	0.64	0.57
Chesapeake	283.89, 36.97	0.45, 1.13	0.43, 0.97	0.94	0.80
Chichijima	142.18, 27.10	0.11, 0.93	0.19, 0.78	0.82	0.64
Churchill	265.80, 58.78	−2.30, −1.54	−1.67, −1.58	−1.74	−1.63
Cordova-B	214.25, 60.56	−0.74, 0.33	−0.60, 0.33	0.18	0.15
Crescent City	235.82, 41.74	0.41, 1.02	0.36, 0.91	0.86	0.75
Cristobal	280.08, 9.36	0.23, 0.78	0.26, 0.69	0.88	0.70
Cuxhaven	8.72, 53.87	0.15, 0.89	0.19, 0.80	0.58	0.53
Darwin	130.85, −12.47	0.21, 0.82	0.19, 0.75	0.70	0.63
Delfzijl	6.93, 53.33	0.17, 0.91	0.20, 0.81	0.60	0.55
Den Helder	4.75, 52.97	0.19, 0.91	0.21, 0.82	0.64	0.58
Dover	1.32, 51.11	0.18, 0.88	0.20, 0.80	0.68	0.61
Draghallan	17.47, 62.33	−1.33, −0.56	−1.04, −0.41	−0.72	−0.58
Eastport	293.01, 44.90	0.35, 1.12	0.31, 0.98	1.03	0.87
Ensenada	243.37, 31.85	0.31, 0.89	0.30, 0.79	0.86	0.73
Esbjerg	8.43, 55.47	0.04, 0.79	0.09, 0.71	0.47	0.44
Esperance	121.90, −33.87	0.22, 0.79	0.22, 0.73	0.66	0.60
Fishguard	355.02, 52.01	0.10, 0.76	0.13, 0.70	0.59	0.53
Fort Denison	151.23, −33.85	0.33, 0.93	0.31, 0.85	0.88	0.79
Fort Pulaski	279.10, 32.03	0.36, 1.03	0.34, 0.90	0.95	0.80
Fremantle	115.73, −32.05	0.17, 0.83	0.19, 0.74	0.66	0.58
Fulford Harbour	236.55, 48.77	−0.05, 0.71	−0.01, 0.65	0.55	0.48
Furuogrund	21.23, 64.92	−1.60, −0.83	−1.28, −0.63	−1.07	−0.86
Galveston	265.21, 29.31	0.33, 0.97	0.33, 0.84	0.75	0.65
Geelong	144.43, −38.17	0.18, 0.76	0.18, 0.71	0.67	0.61
Georgetown	146.85, −41.13	0.33, 0.91	0.29, 0.84	0.78	0.71
Geraldton	114.58, −28.78	0.14, 0.82	0.16, 0.74	0.71	0.62
Goteborg	11.80, 57.68	−0.31, 0.45	−0.20, 0.43	0.24	0.23
Guam	144.65, 13.43	0.25, 0.83	0.28, 0.72	0.80	0.65
Hakodate	140.73, 41.78	0.15, 0.92	0.23, 0.75	0.94	0.67
Halifax	296.42, 44.67	0.49, 1.19	0.42, 1.04	1.06	0.91
Heimsjoe	9.12, 63.43	−0.57, 0.26	−0.42, 0.30	0.10	0.13
Heysham	357.09, 54.03	0.05, 0.71	0.08, 0.66	0.50	0.46
Hilo	204.93, 19.73	0.21, 0.81	0.24, 0.72	0.78	0.65
Hobart	147.33, −42.88	0.35, 0.95	0.31, 0.87	0.83	0.75
Hook of Holland	4.12, 51.98	0.19, 0.91	0.22, 0.82	0.66	0.59
Holyhead	355.37, 53.31	0.07, 0.74	0.10, 0.67	0.57	0.51
Honningsvaag	25.98, 70.98	−0.58, 0.21	−0.42, 0.21	0.07	0.05

Table B1 (*continued*)

Site name	Longitude, latitude (deg.)	Projection 1990–2100 5,95% (m)	Projection 2010–2100 5,95% (m)	Allowance 1990–2100 (m)	Allowance 2010–2100 (m)
Honolulu-B	202.13, 21.31	0.18, 0.81	0.21, 0.73	0.81	0.68
Hosojima	131.68, 32.42	0.23, 0.83	0.24, 0.75	0.68	0.60
Ilha Fiscal	316.83, −22.90	0.16, 0.76	0.17, 0.68	0.60	0.52
Immingham	359.81, 53.63	0.13, 0.84	0.15, 0.76	0.59	0.54
Ishigaki	124.15, 24.33	0.28, 0.86	0.27, 0.77	0.70	0.62
Johnston	190.47, 16.74	0.24, 0.82	0.27, 0.71	0.73	0.61
Kahului	203.53, 20.90	0.19, 0.81	0.21, 0.73	0.86	0.71
Ketchikan	228.38, 55.33	−0.22, 0.52	−0.16, 0.49	0.33	0.30
Key West	278.19, 24.55	0.28, 0.87	0.27, 0.77	0.86	0.72
Klagshamn	12.90, 55.52	−0.04, 0.70	0.03, 0.64	0.45	0.41
Kungsholmsfort	15.58, 56.10	−0.22, 0.53	−0.12, 0.50	0.31	0.30
Kushimoto	135.78, 33.47	0.26, 0.85	0.26, 0.76	0.73	0.64
Kushiro	144.38, 42.97	0.14, 0.80	0.18, 0.75	0.80	0.70
Kwajalein	167.73, 8.73	0.19, 0.84	0.21, 0.74	0.90	0.73
La Coruna	351.60, 43.37	0.19, 0.81	0.20, 0.73	0.68	0.60
La Libertad	279.08, −2.20	0.12, 0.72	0.15, 0.66	0.62	0.54
Landsort	17.87, 58.75	−0.63, 0.13	−0.46, 0.16	−0.01	0.02
Lerwick	358.86, 60.16	0.07, 0.82	0.11, 0.75	0.69	0.61
Lewes	284.88, 38.78	0.47, 1.16	0.45, 0.98	0.95	0.80
Los Angeles	241.73, 33.72	0.32, 0.91	0.31, 0.80	0.89	0.75
Lower Escuminac	295.12, 47.08	0.18, 0.98	0.16, 0.86	0.77	0.66
Lowestoft	1.75, 52.48	0.17, 0.87	0.19, 0.79	0.62	0.56
Maaloey	5.12, 61.93	−0.29, 0.50	−0.18, 0.47	0.32	0.29
Magueyes Island	292.95, 17.97	0.22, 0.77	0.25, 0.69	0.74	0.63
Maisaka	137.62, 34.68	0.26, 0.86	0.27, 0.78	0.69	0.61
Majuro	171.37, 7.11	0.19, 0.83	0.22, 0.73	0.89	0.71
Malakal-A	134.48, 7.33	0.19, 0.87	0.22, 0.76	0.84	0.68
Malin Head	352.67, 55.37	0.05, 0.79	0.08, 0.72	0.64	0.57
Mayport	278.57, 30.39	0.32, 0.98	0.31, 0.86	0.94	0.78
Mera	139.83, 34.92	0.29, 0.86	0.28, 0.78	0.78	0.70
Midway	182.63, 28.22	0.21, 0.86	0.24, 0.75	0.70	0.60
Milford Haven	354.99, 51.70	0.13, 0.79	0.15, 0.72	0.63	0.56
Miyakejima	139.48, 34.06	0.29, 0.86	0.28, 0.79	0.67	0.61
Mokuoloe	202.20, 21.43	0.18, 0.81	0.21, 0.73	0.84	0.70
Montauk	288.04, 41.05	0.42, 1.11	0.40, 0.94	0.90	0.75
Monterey	238.11, 36.60	0.33, 0.93	0.31, 0.82	0.86	0.73
Nagasaki	129.87, 32.73	0.26, 0.83	0.26, 0.75	0.77	0.67
Naha	127.67, 26.22	0.28, 0.90	0.27, 0.80	0.83	0.70
Nantucket	289.90, 41.28	0.45, 1.12	0.43, 0.95	0.95	0.79
Nawiliwili	200.65, 21.97	0.18, 0.80	0.19, 0.73	0.81	0.69
Naze	129.50, 28.38	0.30, 0.88	0.29, 0.78	0.77	0.66
Neah Bay	235.38, 48.37	0.12, 0.81	0.14, 0.73	0.63	0.55
Newcastle	151.80, −32.92	0.32, 0.92	0.30, 0.84	0.87	0.78
New London	287.91, 41.35	0.40, 1.08	0.38, 0.92	0.86	0.72
Newlyn	354.46, 50.10	0.17, 0.82	0.18, 0.74	0.69	0.61
Newport	288.67, 41.51	0.42, 1.11	0.40, 0.94	0.95	0.79
New Westminster	237.09, 49.20	−0.18, 0.57	−0.12, 0.53	0.35	0.32
New York	285.99, 40.70	0.44, 1.12	0.41, 0.95	0.91	0.77
Nishinoomote	130.99, 30.73	0.29, 0.86	0.29, 0.78	0.80	0.71
Northshields	358.56, 55.01	0.07, 0.78	0.10, 0.72	0.62	0.56
North Sydney	299.75, 46.22	0.39, 1.18	0.34, 1.03	0.99	0.84
Noumea	166.44, −22.29	0.29, 0.85	0.31, 0.75	0.85	0.71
Ofunato	141.72, 39.07	0.25, 0.84	0.28, 0.76	0.81	0.70
Olands Norra Udde	17.10, 57.37	−0.41, 0.34	−0.28, 0.34	0.11	0.13
Oslo	10.75, 59.90	−0.55, 0.21	−0.40, 0.23	−0.01	0.02
Pago Pago	189.32, −14.28	0.20, 0.78	0.19, 0.70	0.80	0.70
Patricia Bay	236.55, 48.65	−0.05, 0.71	−0.01, 0.65	0.53	0.47
Pensacola	272.79, 30.40	0.35, 0.99	0.34, 0.87	0.78	0.68
Pohnpei-B	158.24, 6.99	0.21, 0.82	0.23, 0.73	0.79	0.66
Point Atkinson	236.75, 49.34	−0.16, 0.60	−0.10, 0.55	0.42	0.37
Point Lonsdale	144.62, −38.30	0.18, 0.76	0.18, 0.71	0.65	0.59
Port Adelaide (inner)	138.50, −34.85	0.18, 0.76	0.19, 0.70	0.57	0.53
Port Adelaide (outer)	138.48, −34.78	0.18, 0.76	0.19, 0.70	0.56	0.52
Port-aux-Basques	300.87, 47.57	0.30, 1.09	0.27, 0.96	1.08	0.91
Port Hardy	232.51, 50.72	−0.03, 0.67	0.01, 0.61	0.52	0.45
Port Hedland	118.58, −20.30	0.16, 0.83	0.18, 0.74	0.65	0.57
Portland	289.75, 43.66	0.29, 1.05	0.26, 0.93	0.93	0.79
Port Lincoln	135.87, −34.72	0.21, 0.78	0.21, 0.72	0.63	0.57
Portpatrick	354.88, 54.84	0.05, 0.77	0.08, 0.71	0.57	0.52
Port Pirie	138.02, −33.17	0.17, 0.75	0.18, 0.70	0.54	0.50
Prince Rupert	229.68, 54.32	−0.18, 0.53	−0.12, 0.49	0.32	0.30
Puerto de la Luz	344.58, 28.13	0.19, 0.76	0.22, 0.69	0.67	0.58
Puerto Williams	292.38, −54.93	−0.02, 0.61	0.01, 0.56	0.48	0.43
Queen Charlotte City	227.93, 53.25	0.11, 0.78	0.12, 0.71	0.61	0.54

Table B1 (*continued*)

Site name	Longitude, latitude (deg.)	Projection 1990–2100 5,95% (m)	Projection 2010–2100 5,95% (m)	Allowance 1990–2100 (m)	Allowance 2010–2100 (m)
Ratan	20.92, 64.00	−1.54, −0.77	−1.22, −0.59	−0.99	−0.79
Rikitea	225.05, −23.12	0.13, 0.72	0.17, 0.64	0.80	0.66
Roervik	11.25, 64.87	−0.70, 0.17	−0.53, 0.23	−0.04	0.02
Saint John	293.94, 45.25	0.29, 1.06	0.26, 0.93	0.93	0.79
Salina Cruz	264.80, 16.16	0.15, 0.77	0.21, 0.68	0.75	0.62
San Diego	242.83, 32.71	0.32, 0.90	0.31, 0.80	0.86	0.73
San Francisco	237.53, 37.81	0.35, 0.95	0.32, 0.83	0.82	0.71
Seattle	237.66, 47.60	0.03, 0.79	0.05, 0.71	0.66	0.57
Seward-C	210.57, 60.12	−0.46, 0.47	−0.37, 0.44	0.33	0.29
Sheerness	0.75, 51.44	0.17, 0.87	0.19, 0.79	0.68	0.61
Simon's Bay	18.43, −34.18	0.24, 0.82	0.28, 0.73	0.83	0.68
Sitka	224.66, 57.05	−0.26, 0.53	−0.19, 0.49	0.40	0.35
Smogen	11.22, 58.37	−0.46, 0.29	−0.33, 0.30	0.12	0.12
Socoa	358.32, 43.40	0.15, 0.79	0.17, 0.72	0.66	0.59
South Beach	235.96, 44.62	0.43, 1.06	0.39, 0.94	0.87	0.76
Spikarna	17.53, 62.37	−1.33, −0.56	−1.04, −0.41	−0.80	−0.63
St. Johns	307.28, 47.57	0.41, 1.13	0.34, 1.00	1.08	0.93
Stockholm	18.08, 59.32	−0.84, −0.09	−0.64, −0.02	−0.24	−0.18
St. Petersburg	277.37, 27.76	0.32, 0.94	0.31, 0.83	0.76	0.66
Thevenard	133.65, −32.15	0.19, 0.76	0.20, 0.70	0.59	0.54
Tofino	234.09, 49.15	−0.03, 0.70	0.01, 0.63	0.53	0.46
Townsville	146.83, −19.25	0.24, 0.81	0.24, 0.74	0.66	0.59
Toyama	137.22, 36.77	0.20, 0.90	0.26, 0.76	0.93	0.70
Tregde	7.57, 58.00	−0.26, 0.49	−0.16, 0.47	0.35	0.31
Truk	151.85, 7.45	0.20, 0.84	0.23, 0.74	0.82	0.67
Tumaco	281.27, 1.83	0.15, 0.71	0.17, 0.65	0.62	0.54
Ullapool	354.84, 57.90	0.04, 0.76	0.09, 0.69	0.58	0.52
Valparaiso	288.37, −33.03	0.04, 0.66	0.08, 0.60	0.63	0.54
Vancouver	236.89, 49.29	−0.16, 0.60	−0.10, 0.55	0.44	0.39
Varberg	12.22, 57.10	−0.33, 0.42	−0.21, 0.41	0.21	0.21
Vardo	31.10, 70.33	−0.57, 0.24	−0.42, 0.24	0.14	0.11
Victor Harbor	138.63, −35.57	0.19, 0.77	0.20, 0.72	0.61	0.56
Victoria	236.63, 48.42	−0.05, 0.71	−0.01, 0.65	0.51	0.45
Vigo	351.27, 42.23	0.18, 0.79	0.19, 0.72	0.63	0.57
Wake	166.62, 19.28	0.19, 0.81	0.24, 0.70	0.73	0.60
Wakkanai	141.68, 45.42	0.07, 0.67	0.11, 0.63	0.59	0.53
Walvis Bay	14.50, −22.95	0.20, 0.77	0.25, 0.68	0.65	0.55
Wellington	174.78, −41.28	0.31, 0.91	0.30, 0.80	0.88	0.74
Wick	356.91, 58.44	0.06, 0.80	0.09, 0.74	0.64	0.58
Williamstown	144.92, −37.87	0.17, 0.75	0.17, 0.70	0.61	0.56
Wilmington	282.05, 34.23	0.39, 1.06	0.37, 0.91	0.89	0.75
Wladyslawowo	18.42, 54.80	0.02, 0.76	0.08, 0.69	0.54	0.48
Wood Islands	297.30, 45.68	0.42, 1.22	0.36, 1.06	0.98	0.84
Woods Hole	289.33, 41.52	0.45, 1.12	0.43, 0.95	0.91	0.76
Wyndham	128.10, −15.45	0.18, 0.81	0.16, 0.74	0.76	0.68
Xiamen	118.07, 24.45	0.21, 0.78	0.20, 0.72	0.59	0.54
Yakutat	220.26, 59.55	−0.86, 0.25	−0.69, 0.26	0.16	0.12
Yap-B	138.13, 9.51	0.23, 0.84	0.24, 0.75	0.67	0.59
Yarmouth	293.88, 43.83	0.42, 1.19	0.37, 1.04	1.07	0.91
Ystad	13.82, 55.42	−0.06, 0.69	0.01, 0.63	0.47	0.42

References

Bindoff, N., Willebrand, J., Artale, V., Cazenave, A., Gregory, J., Gulev, S., Hanawa, K., Quéré, C.L., Levitus, S., Nojiri, Y., Shum, C., Talley, L., Unnikrishnan, A., 2007. Observations: oceanic climate change and sea level. In: Solomon, S., Qin, D., Manning, M., Chen, Z., Marquis, M., Averyt, K., Tignor, M., Miller, H. (Eds.), Climate Change 2007: The Physical Science Basis. Contribution of Working Group I to the Fourth Assessment Report of the Intergovernmental Panel on Climate Change. Cambridge University Press, Cambridge, United Kingdom and New York, NY, USA, pp. 385–432 (Chapter 5).

van den Brink, H., Können, G., 2011. Estimating 10,000-year return values from short time series. Int. J. Climatol. 31, 115–126, http://dx.doi.org/10.1002/joc.2047.

Church, J., White, N., 2011. Sea-level rise from the late 19th to the early 21st century. Surv. Geophys. 32 (4–5), 585–602, http://dx.doi.org/10.1007/s10712-011-9119-1.

Church, J., Gregory, J., White, N., Platten, S., Mitrovica, J., 2011. Understanding and projecting sea level change. Oceanography 24 (2), 130–143, http://dx.doi.org/10.5670/oceanog.2011.33.

Coles, S., 2001. An Introduction to Statistical Modeling of Extreme Values. Springer-Verlag, London, Berlin, Heidelberg.

Hunter, J., 2012. A simple technique for estimating an allowance for uncertain sea-level rise. Climatic Change 113, 239–252, http://dx.doi.org/10.1007/s10584-011-0332-1.

IPCC, 2007. Summary for policymakers. In: Solomon, S., Qin, D., Manning, M., Chen, Z., Marquis, M., Averyt, K., Tignor, M., Miller, H. (Eds.), Climate Change 2007: The Physical Science Basis. Contribution of Working Group I to the Fourth Assessment Report of the Intergovernmental Panel on Climate Change. Cambridge University Press, Cambridge, United Kingdom and New York, NY, USA, pp. 1–18.

ISO, 2009. 31000:2009 Risk Management—Principles and Guidelines. International Organisation for Standardization. 〈www.iso.org〉.

Kendall, R., Mitrovica, J., Milne, G., 2005. On post-glacial sea level: II. Numerical formulation and comparative results on spherically symmetric models. Geophys. J. Int. 161 (3), 679–706, http://dx.doi.org/10.1111/j.1365-246X.2005.02553.x.

Le Quéré, C., Raupach, M., Canadell, J., Marland, G., et al., 2009. Trends in the sources and sinks of carbon dioxide. Nat. Geosci. 2, 831–836, http://dx.doi.org/10.1038/ngeo689.

Lemke, P., Ren, J., Alley, R., Allison, I., Carrasco, J., Flato, G., Fujii, Y., Kaser, G., Mote, P., Thomas, R., Zhang, T., 2007. Observations: changes in snow, ice and frozen ground. In: Solomon, S., Qin, D., Manning, M., Chen, Z., Marquis, M., Averyt, K., Tignor, M., Miller, H. (Eds.), Climate Change 2007: The Physical Science Basis. Contribution of Working Group I to the Fourth Assessment Report of the

Intergovernmental Panel on Climate Change. Cambridge University Press, Cambridge, United Kingdom and New York, NY, USA, pp. 337–383 (Chapter 4).

Lowe, J., Woodworth, P., Knutson, T., McDonald, R., McInnes, K., Woth, K., Von Storch, H., Wolf, J., Swail, V., Bernier, N., Gulev, S., Horsburgh, K., Unnikrishnan, A., Hunter, J., Weisse, R., 2012. Past and future changes in extreme sea levels and waves. In: Church, J., Woodworth, P., Aarup, T., Wilson, S. (Eds.), Understanding Sea-Level Rise and Variability. Wiley-Blackwell, Oxford, United Kingdom, pp. 326–375 (Chapter 11).

Maaskant, B., Jonkman, S., Bouwer, L., 2009. Future risk of flooding: an analysis of changes in potential loss of life in South Holland (The Netherlands). Environ. Sci. Policy 12, 157–169, http://dx.doi.org/10.1016/j.envsci.2008.11.004.

McInnes, K., Macadam, I., Hubbert, G., O'Grady, J., 2009. A modelling approach for estimating the frequency of sea level extremes and the impact of climate change in southeast Australia. Nat. Hazards 51, 115–137, http://dx.doi.org/10.1007/s11069-009-9383-2.

Meehl, G., Stocker, T., Collins, W., Friedlingstein, P., Gaye, A., Gregory, J., Kitoh, A., Knutti, R., Murphy, J., Noda, A., Raper, S., Watterson, I., Weaver, A., Zhao, Z.C., 2007. Global climate projections. In: Solomon, S., Qin, D., Manning, M., Chen, Z., Marquis, M., Averyt, K., Tignor, M., Miller, H. (Eds.), Climate Change 2007: The Physical Science Basis. Contribution of Working Group I to the Fourth Assessment Report of the Intergovernmental Panel on Climate Change. Cambridge University Press, Cambridge, United Kingdom and New York, NY, USA, pp. 747–845 (Chapter 10).

Menéndez, M., Woodworth, P., 2010. Changes in extreme high water levels based on a quasi-global tide-gauge data set. J. Geophys. Res. 115 (C10011), http://dx.doi.org/10.1029/2009JC005997.

Mitrovica, J., Tamisiea, M., Davis, J., Milne, G., 2001. Recent mass balance of polar ice sheets inferred from patterns of global sea-level change. Nature 409 (6823), 1026–1029, http://dx.doi.org/10.1038/35059054.

Mitrovica, J., Gomez, N., Morrow, E., Hay, C., Latychev, K., Tamisiea, M., 2011. On the robustness of predictions of sea level fingerprints. Geophys. J. Int. 187, 729–742, http://dx.doi.org/10.1111/j.1365-246X.2011.05090.x.

Nakicenovic, N., Alcamo, J., Davis, G., de Vries, B., Fenhann, J., Gaffin, S., Gregory, K., Griibler, A., Jung, T., Kram, T., La Rovere, E., Michaelis, L., Mori, S., Morita, T., Pepper, W., Pitcher, H., Price, L., Riahi, K., Roehrl, A., Rogner, H., Sankovski, A., Schlesinger, M., Shukla, P., Smith, S., Swart, R., van Rooijen, S., Victor, N., Dadi, Z., 2000. Special Report on Emissions Scenarios. A Special Report of Working Group III of the Intergovernmental Panel on Climate Change. Cambridge University Press, Cambridge, UK.

Nordhaus, W., 2011. The economics of tail events with an application to climate change. Rev. Environ. Econ. Policy 5 (2), 240–257.

Pfeffer, W., Harper, J., O'Neel, S., 2008. Kinematic constraints on glacier contributions to 21st-century sea-level rise. Science 321 (5894), 1340–1343, http://dx.doi.org/10.1126/science.1159099.

Pickering, M., Wells, N., Horsburgh, K., Green, J., 2012. The impact of future sea-level rise on the European Shelf tides. Cont. Shelf Res. 35, 1–15, http://dx.doi.org/10.1016/j.csr.2011.11.011.

Pindyck, R., 2011. Fat tails, thin tails, and climate change policy. Rev. Environ. Econ. Policy 5 (2), 258–274.

Pugh, D., 1996. Tides, Surges and Mean Sea-Level. John Wiley & Sons, reprinted with corrections, 〈http://eprints.soton.ac.uk/19157/01/sea-level.pdf〉, Chichester, New York, Brisbane, Toronto and Singapore.

R Development Core Team, 2008. R: A Language and Environment for Statistical Computing. R Foundation for Statistical Computing, Vienna, Austria, URL 〈http://www.R-project.org〉, ISBN 3-900051-07-0.

Slangen, A., Katsman, C., van de Wal, R., Vermeersen, L., Riva, R., 2012. Towards regional projections of twenty-first century sea-level change based on IPCC SRES scenarios. Climate Dyn. 38, 1191–1209, http://dx.doi.org/10.1007/s00382-011-1057-6.

Weitzman, M., 2009. On modeling and interpreting the economics of catastrophic climate change. Rev. Econ. Stat. 91 (1), 1–19.

Woodworth, P., Blackman, D., 2004. Evidence for systematic changes in extreme high waters since the mid-1970s. J. Climate 17 (6), 1190–1197, http://dx.doi.org/10.1175/1520-0442(2004)017 < 1190:EFSCIE > 2.0.CO;2.